Optics Communications 324 (2014) 221–226

Contents lists available at ScienceDirect

Optics Communications

journal homepage: www.elsevier.com/locate/optcom

Phase control of group velocity via Fano-type interference in a triple semiconductor quantum well

Wen-Xing Yang [a,b,*], Wen-Hai Ma [a], Long Yang [a], Guo-Rui Zhang [a], Ray-Kuang Lee [b]

[a] Department of Physics, Southeast University, Nanjing 210096, China
[b] Institute of Photonics Technologies, National Tsing-Hua University, Hsinchu 300, Taiwan

ARTICLE INFO

Article history:
Received 19 January 2014
Received in revised form
15 March 2014
Accepted 23 March 2014
Available online 3 April 2014

Keywords:
Subluminal
Superluminal
Quantum interference
Semiconductor quantum well

ABSTRACT

We analyze the absorption-dispersive properties of a weak probe laser field based on the ISBT in a triple semiconductor quantum well (SQW) structure driven coherently by two control laser fields. It is shown that the system can produce anomalous and normal dispersion regions with negligible absorption by adjusting the intensities of the control fields and the Fano-type interference. More interestingly, the dispersion can be changed between normal and anomalous simply by adjusting the relative phase between two coherent control fields due to the existence of the Fano-type interference. Thus the relative phase can be regarded as a switch to manipulate light propagation with subluminal or superluminal. In addition, the temporal and spatial dynamics of the probe laser pulse with Gaussian-type envelope are analyzed.

1. Introduction

In the past few decades, much attention has been paid to controlling the group velocity of light pulses [1–13] due to the potential applications in optical communications and quantum information processing. Especially, subluminal and superluminal propagations of the light pulses have gained considerable interest for their wide applications from optical clock distribution, beam steering to radio frequency (RF) phased array antennas, and realizing an all-optical buffer [14]. Recently, the subluminal and superluminal phenomena have been observed in many fields of physics, such as cold atomic vapor and alexandrite crystal. Many experimental observations are based on the fact that quantum coherence and interference [15,16] lead to a dispersion profile with a sharp derivative (positive or negative) near the line center [17]. On the other hand, optical transitions between electronic states within the conduction bands of semiconductor quantum wells (SQW) have proved to be a promising candidate for the realization of optical devices and solid quantum information sciences [18,19], and large number of efforts has been devoted to the investigations of both quantum coherence and interference in quantum wells.

Due to strong electron–electron interactions, the two-dimensional electron gas behaves effectively as a single oscillator with atomic-like intersubband transition (ISBT) responses [18]. In these solid-state systems, the large intrinsic dipole matrix elements may give rise to a fast Rabi oscillation in the time domain, which allows coherent processes to occur on the time scales shorter than the typical ISBT dipole dephasing time. Moreover, the ISBT energies and electron wave-function symmetries can be engineered. Due to this unique flexibility, which can be hardly found in other systems, a large number of theoretical schemes have been proposed and some experimental realizations have been reported, such as gain without inversion [20–23], coherently controlled photocurrent generation [24], electromagnetically induced transparency [25], slow light [26], quantum interference and coherence [27–31], optical bistability [32–34], photon switch [35–37] and solitons [38–40].

It is usually believed that the population decay process for intersubbands due to longitudinal optical phonon emission can destroy the coherent properties. Nevertheless, population decay can be used to produce quantum interference between the discrete state and continuum component in SQW systems [20,21]. This kind of interference is called Fano-type interference [20,21], which will lead to nonreciprocal absorptive and dispersive profiles. More recently, we have also studied the slow optical soliton formations based on the Fano interference with a three-level system of electronic subbands in an asymmetric double quantum well (GaAs/AlGaAs) structure in which the interference between the absorption paths through two resonances to the continuum leads to a linear rapidly varying refractive index change with a reduction in the group velocity [38]. Besides, we should note that the relative phase of applied laser fields has been widely used for the coherent control of ISBT in SQW systems [41].

* Corresponding author. Tel.: +86 25 52090605-8407
E-mail address: wenxingyang@seu.edu.cn (W.-X. Yang).

http://dx.doi.org/10.1016/j.optcom.2014.03.071
0030-4018/

This method, which is called phase control, has been applied for the coherent manipulation of population dynamics and absorption-dispersive properties in SQW systems [42]. All the mentioned characteristics offer a feasible platform for the realization of phase control of the group velocity.

In this paper, we analyze the absorption-dispersive properties of a weak probe laser field based on the ISBT in a triple semiconductor quantum well (SQW) structure driven coherently by two control laser fields. It is shown that the absorption-dispersive properties of the probe field can be controlled efficiently through the intensities of the two control fields and the Fano-type interference. Due to the existence of the Fano-type interference, the dispersion and the absorption are very sensitive to the relative phase between two coherent control fields, and the dispersion can be changed between normal and anomalous simply by adjusting this relative phase. This leads to the group velocity of the probing field switching between subluminal and superluminal. Our results illustrate the potential to utilize relative phase of the coherent fields for controlling group velocity of the light pulse in SQW systems, as well as a guidance in the design for possible experimental implementations.

2. The system and the density matrix equations

As shown in Fig. 1, the proposed quantum well structure includes a deep well and two shallow wells coupled by tunneling to a common continuum of energies through a thin barrier. This triple SQW band structure and related level configurations are shown in Fig. 1(a) and (b), respectively. The present SQW structure is the same as that in Ref. [22] and it can be obtained by coupling two shallow 6.8-nm-thick $Al_{0.2}Ga_{0.8}As$ wells separated by a 2.0-nm -thick $Al_{0.4}Ga_{0.6}As$ barrier and a deep 7.1-nm-thick GaAs well to a common continuum ($Al_{0.165}Ga_{0.835}As$) through a 0.7-nm-thick $Al_{0.4}Ga_{0.6}As$ Al barrier. The deep well and its adjacent shallow well are separated by an $Al_{0.4}Ga_{0.6}As$ barrier 2.5 nm thick. The electronic wave functions of the ground state of deep well and three excited states are denoted by $|1\rangle$, $|2\rangle$, $|3\rangle$, and $|4\rangle$. A probe field with Rabi frequency Ω_p and angular frequency ω_p is applied to the transition $|1\rangle\leftrightarrow|2\rangle$; while the transitions $|1\rangle\leftrightarrow|3\rangle$ and $|1\rangle\leftrightarrow|4\rangle$ are mediated by coherent control fields with Rabi frequency Ω_c and angular frequency ω_c and Rabi frequency Ω_L and angular frequency ω_L.

By adopting the standard approach [18], the density-matrix equations of motion in dipole and rotating-wave approximations for this system can be written as follows:

$$i\frac{\partial\rho_{33}}{\partial t}=i\gamma_3\rho_{11}+\Omega_c e^{i\phi}\rho_{13}-\Omega_c^* e^{-i\phi}\rho_{31} -i\kappa_{23}(\rho_{23}+\rho_{32})-i\kappa_{43}(\rho_{34}+\rho_{43}) \tag{1}$$

$$i\frac{\partial\rho_{22}}{\partial t}=-i(\gamma_2+\gamma_3+\gamma_4)\rho_{11}+\Omega_p^*\rho_{21}-\Omega_p\rho_{12}+\Omega_c^* e^{-i\phi}\rho_{31} -\Omega_c e^{i\phi}\rho_{13}+\Omega_L^* e^{i\phi}\rho_{41}-\Omega_L e^{-i\phi}\rho_{14} \tag{2}$$

$$-i\kappa_{24}(\rho_{24}+\rho_{42})-i\kappa_{32}(\rho_{32}+\rho_{23}) \tag{3}$$

$$i\frac{\partial\rho_{41}}{\partial t}=(\Delta_L-i\gamma_{41})\rho_{41}+\Omega_L e^{-i\phi}(\rho_{11}-\rho_{44}) -\Omega_p\rho_{42}-\Omega_c e^{i\phi}\rho_{43}-i\kappa_{43}\rho_{13}-i\kappa_{24}\rho_{21} \tag{4}$$

$$i\frac{\partial\rho_{24}}{\partial t}=(\Delta_L-\Delta_p-i\gamma_{24})\rho_{24}-\Omega_L^*\rho_{21}e^{i\phi}+\Omega_p\rho_{14}-i\kappa_{43}\rho_{23}-i\kappa_{32}\rho_{43} \tag{5}$$

$$i\frac{\partial\rho_{43}}{\partial t}=(\Delta_L-\Delta_c-i\gamma_{43})\rho_{43}+\Omega_L e^{-i\phi}\rho_{13} -\Omega_c^* e^{-i\phi}\rho_{41}-i\kappa_{32}\rho_{24}-i\kappa_{24}\rho_{23} \tag{6}$$

$$i\frac{\partial\rho_{23}}{\partial t}=(\Delta_c-\Delta_p-i\gamma_{23})\rho_{23}-\Omega_c^*\rho_{21}e^{-i\phi}+\Omega_p\rho_{13}-i\kappa_{24}\rho_{43}-i\kappa_{43}\rho_{24} \tag{7}$$

$$i\frac{\partial\rho_{13}}{\partial t}=(\Delta_c-i\gamma_{13})\rho_{13}-\Omega_c^* e^{-i\phi}(\rho_{11}-\rho_{33})+\Omega_p^*\rho_{23} +\Omega_L^* e^{-i\phi}\rho_{43}-i\kappa_{32}\rho_{21}-i\kappa_{43}\rho_{41} \tag{8}$$

$$i\frac{\partial\rho_{21}}{\partial t}=(\Delta_p-i\gamma_{21})\rho_{21}+\Omega_c e^{i\phi}\rho_{23}+\Omega_p(\rho_{11}-\rho_{22}) -\Omega_L\rho_{23}-\Omega_L\rho_{24}e^{-i\phi}-i\kappa_{32}\rho_{13}-i\kappa_{24}\rho_{41} \tag{9}$$

with $\rho_{ij}=\rho_{ji}^*$ $(i,j=1,2,3,4;i\neq j)$. Actually, these density matrix equations (1–9) are to be supplemented by the population conservation condition, $\rho_{11}+\rho_{22}+\rho_{33}+\rho_{44}=1$. The half Rabi frequencies associated with the field driving the transitions are defined as $\Omega_k=\mu_{ij}E_k/2\hbar$ $i,j=1,2,3,4$, $i\neq j$, and $k=p,c,L$), with E_k and μ_{ij} being the corresponding electric field amplitude and the relative dipole matrix element induced on the transition $|i\rangle\leftrightarrow|j\rangle$,

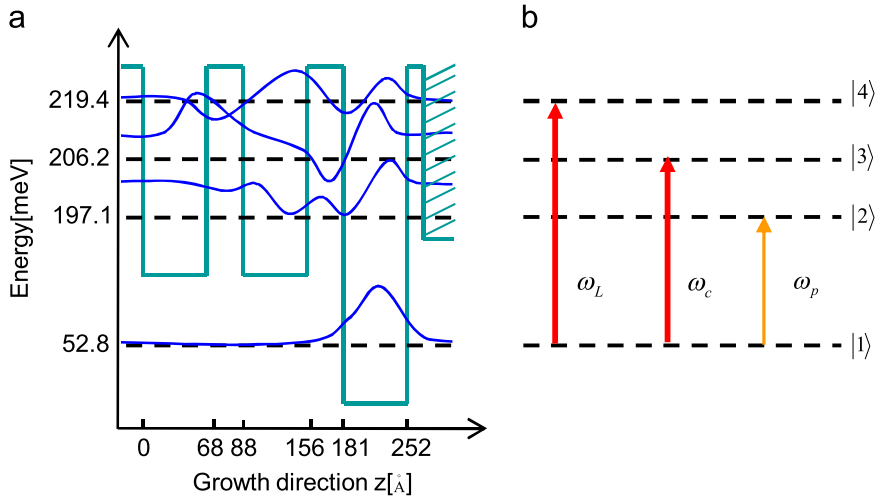

Fig. 1. (a) Schematic band diagram of the SQW structure consisting of a deep well and two shallow wells coupled by tunneling to a common continuum of energies through a thin barrier. The ground states of two shallow wells and the first excited state of the deep well mix to create three excited states of the system. Related energy level and the corresponding wave functions are denoted by dashed and solid lines, respectively. (b) Schematic of related energy levels, where electronic wave functions of the ground state of deep well and three excited states are labeled as $|1\rangle$, $|2\rangle$, $|3\rangle$, and $|4\rangle$.

respectively. $\phi=\phi_c-\phi_L$ is the relative phase between the two control fields, which only depends on the initial phases (ϕ_c,ϕ_L) of the two control fields. $\Delta_p=(\varepsilon_2-\varepsilon_1)/\hbar-\omega_p$, $\Delta_c=(\varepsilon_3-\varepsilon_1)/\hbar-\omega_c$ and $\Delta_L=(\varepsilon_4-\varepsilon_1)/\hbar-\omega_L$ are the detunings of probe field and two coherent control fields, respectively, and $\varepsilon_j(j=1\text{–}4)$ is the energy of state $|j\rangle$. The decay rates are included phenomenologically in the above equations. The total decay rates $\gamma_{ij}(i\neq j)$ are given by $\gamma_{21}=(\gamma_2+\gamma_{21}^{dph})/2$, $\gamma_{32}=(\gamma_2+\gamma_3+\gamma_{32}^{dph})/2$, $\gamma_{31}=(\gamma_3+\gamma_{31}^{dph})/2$, $\gamma_{41}=(\gamma_4+\gamma_{41}^{dph})/2$, $\gamma_{42}=(\gamma_2+\gamma_4+\gamma_{42}^{dph})/2$, and $\gamma_{43}=(\gamma_3+\gamma_4+\gamma_{43}^{dph})/2$, where the population scattering rates $\gamma_j(j=2,3,4)$ are primarily due to the longitudinal optical phonon emission events at low temperature [43] and the pure dipole dephasing rates γ_{ij}^{dph} are assumed to be a combination of quasi-elastic interface roughness scattering or acoustic phonon scattering [23,29,44]. The population decay rates can be calculated by solving the effective mass Schrodinger equation. For the temperatures up to 10 K, the dephasing decay rates γ_{ij}^{dph} can be estimated according to Refs. [22,45,46]. For our SQW system considered, they turn out to be $\gamma_2=1.32$ meV, $\gamma_3=1.72$ meV, $\gamma_4=2.24$ meV, and $\gamma_{21}^{dph}=\gamma_{31}^{dph}=\gamma_{41}^{dph}=\gamma_{32}^{dph}=\gamma_{42}^{dph}=\gamma_{43}^{dph}=1.65$ meV. A comprehensive treatment of the decay rates would involve incorporation of the decay mechanisms into the Hamiltonian of the system. However, we have adopted the phenomenological approach of treating the decay mechanisms just as done in Ref. [18–44]. A more fully two-dimensional treatment taking into account these processes has been investigated quite thoroughly by some authors (for example [47,48]). $\kappa_{ij}=(p/2)\sqrt{\gamma_{i1}\gamma_{j1}}$ denotes a cross coupling term between the excited states $|i\rangle$ and $|j\rangle$, due to the Fano-type interference in the electronic continuum [21]. It is noted that p represents the strength of Fano-type interference, where the values $p=0$ and $p=1$ correspond to no interference and perfect interference, respectively.

3. Numerical analysis for controlling the group velocity

In this section, we mainly focus on controlling the group velocity of the weak probe field applied to the transition $|1\rangle\leftrightarrow|2\rangle$. The group velocity is defined by $v_g=c/n_g$ with n_g and c being the group refractive index and vacuum light speed, respectively. n_g is related to the susceptibility χ_{21} for the transition $|1\rangle\leftrightarrow|2\rangle$ as follows:

$$n_g=1+\frac{1}{2}\chi'_{21}+\frac{1}{2}\omega_p\frac{\partial\chi'_{21}}{\partial\omega_p}, \tag{10}$$

where χ'_{21} is the real part of χ_{21}, which is related with ρ_{21} by

$$\chi_{21}=\frac{2N|\mu_{21}|^2}{\hbar\varepsilon_0\Omega_p}\rho_{21}(t), \tag{11}$$

where N is the electron density in the conduction band of quantum well and ε_0 is the vacuum dielectric constant. Our main interest is the dispersion and the gain-absorption characteristics of the probe field, from which we can simply demonstrate the possible effects of the relative phase, the control fields and the Fano-type interference on the group velocity. When the dispersion curve is very steep and normal, the group velocity is significantly reduced and the subluminal exhibits. On the other hand, when the dispersion is anomalous and steep, the group velocity is increased or even becomes negative and the superluminal exhibits. In the limit of a weak probe, the dispersion and gain-absorption coefficients for the probe field are governed by the real and imaginary parts of the susceptibility $\chi_{21}\propto\rho_{21}(t)$. In the following, we will directly examine the transient dispersion–absorption property of the weak probe field by numerically integrating Eqs. (1–9) with a given initial condition. With the initial conditions $\rho_{11}(0)=1$, $\rho_{22,33,44}(0)=0$ and $\rho_{ij}(0)=0$ for $i\neq j$ $(i,j=1,2,3,4)$, we solve the time-dependent equations (1–9) by a standard fourth-order Runge–Kutta method.

First of all, we analyze the effects of intensities of two control fields on the dispersion and gain-absorption properties of the probe field in this SQW system. The detuning of the fields, the strength of Fano-type interference, the relative phase and the intensity of the probe fields are $\Delta_L=\Delta_c=0$, $p=0.9$, $\phi=0$ and $\Omega_p=0.1$ meV, respectively. We plot in Fig. 2 the real and imaginary parts of ρ_{21} as a function of the detuning Δ_p for different values of Ω_c and Ω_L with fixed relative phase (i.e., $\phi=0$). The parameters are chosen as (a) $\Omega_L=\Omega_c=\Omega=1.5$ meV; (b) $\Omega_L=\Omega_c=\Omega=10$ meV. As shown in Fig. 2, the susceptibility of the probe field depends so sensitively on the Rabi energies of the two control fields that the corresponding profiles are quite different. Specifically, as shown in Fig. 2(a), a positive steep dispersion can be observed and is accompanied by a transparency window around $\Delta_p=0$ between two absorption lines. The positive dispersion curve corresponds to a normal dispersion and leads to a slowing down of the group velocity. Contrarily, as shown in Fig. 2(b), the real susceptibility for the probe exhibits anomalous dispersion accompanied by transparency at $\Delta_p=0$ between two closely spaced gain line, and superluminal behavior occurs. That is, the group velocity of the probe field can be changed from subluminal group velocity to superluminal group velocity by varying the intensities of the control fields. Therefore, the control fields can be used as a switching to manipulate the group velocity of the probe field. And this optical switching provides an efficient and convenient way to achieve slow- and fast-light.

Similarly, the effects of the strength or quality of the Fano-type interference on the dispersion–absorption responses of the probe field are illustrated in Fig. 3. The strength of the Fano-type interference is chosen as (a) $p=0.1$; (b) $p=0.8$. As can be seen from Fig. 3, the susceptibility of the probe field also depends sensitively on the parameter p. For the case $p=0.1$, the absorption-gain curve exhibits two gain peaks with a transparency window at probing resonance $\Delta_p=0$. The dispersion presents steep and positive slope for the probe filed, which leads to subluminal propagation of the probe field. However, for the case $p=0.8$, the curves of the Fig. 3(b) exhibit a negative slope accompanied by negligible absorption around probing resonance, which corresponds to superluminal propagation of the probe field. More interestingly, the parameters of the electron subbands in SQW structures can be engineered to give a desired strength of interference by utilizing the so-called structure coherent control in design [18]. Thus we may provide a new method to manipulate the group velocity and the gain-absorption of the probe field in solid-state system.

We should consider the relative phase ϕ between the two control fields, which is one of the most interesting characters of this SQW system. We show in Fig. 4(a) and (b) the variations of the real and imaginary parts of ρ_{21} versus the probe detuning Δ_p with different values of ϕ without including the Fano interference (i.e., $p=0$). The relative phase between the two control fields is chosen as 4(a) $\phi=0$; 4(b) $\phi=\pi$. Both Fig. 4(a) and (b) show that a positive and steep dispersion with a transparency window at probing resonance between two gain peaks. The positive dispersion corresponds to a subluminal propagation of the probe field. From Fig. 4(a) and (b), one can find that the effect of the relative phase on the dispersion can be ignored when the effect of Fano interference is not considered, i.e., in this case, we cannot manipulate the group velocity of the weak probing pulse from subluminal to superluminal or vice versa by adjusting the relative phase ϕ. By including the Fano interference (i.e., $p=0.9$), we plot in Fig. 4 (c) and (d) the real and imaginary parts of ρ_{21} versus the probe detuning, respectively. As shown in Fig. 4(c), a negative and steep

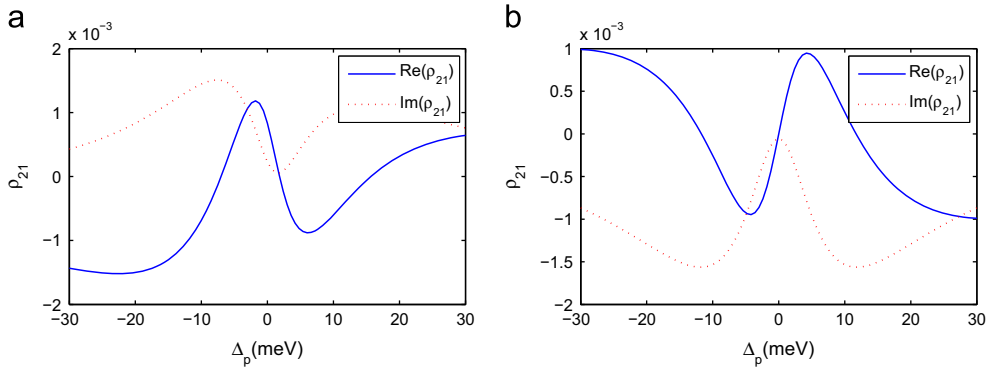

Fig. 2. The real (solid line) and imaginary (dotted line) parts of ρ_{21} as a function of the detuning of the probe field Δ_p with different intensities of the two control fields: (a) $\Omega_L=\Omega_c=1.5$ meV; (b) $\Omega_L=\Omega_c=\Omega=10$ meV. The other values of the parameters are chosen as $\phi=0$, $\Delta_L=\Delta_c=0$, $\gamma_2=1.32$ meV, $\gamma_3=1.72$ meV, $\gamma_4=2.24$ meV, $\gamma_{21}^{dph}=\gamma_{31}^{dph}=\gamma_{41}^{dph}=\gamma_{32}^{dph}=\gamma_{42}^{dph}=\gamma_{43}^{dph}=1.65$ meV, $p=0.9$ and $\Omega_p=0.1$ meV.

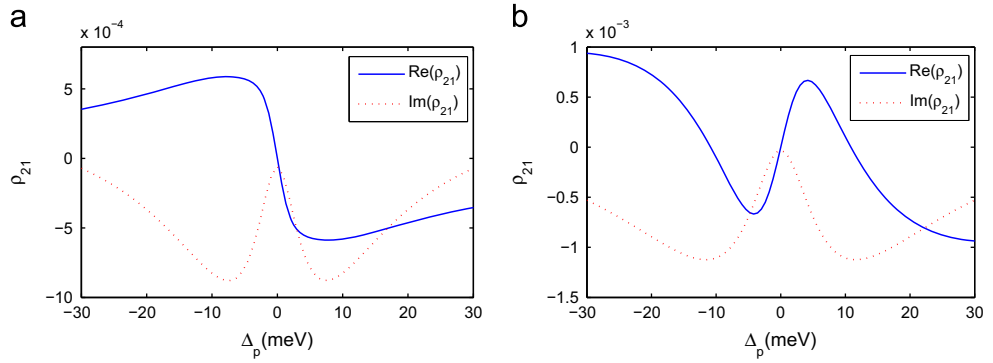

Fig. 3. The real (solid line) and imaginary (dotted line) parts of ρ_{21} as a function of the detuning of the probe field Δ_p with different strength of the Fano-type interference: (a) $p=0.1$; (b) $p=0.8$. The other values of the parameters are chosen as $\phi=0$, $\Delta_L=\Delta_c=0$, $\gamma_2=1.32$ meV, $\gamma_3=1.72$ meV, $\gamma_4=2.24$ meV, $\gamma_{21}^{dph}=\gamma_{31}^{dph}=\gamma_{41}^{dph}=\gamma_{32}^{dph}=\gamma_{42}^{dph}=\gamma_{43}^{dph}=1.65$ meV, $\Omega_L=\Omega_c=\Omega=10$ meV and $\Omega_p=0.1$ meV.

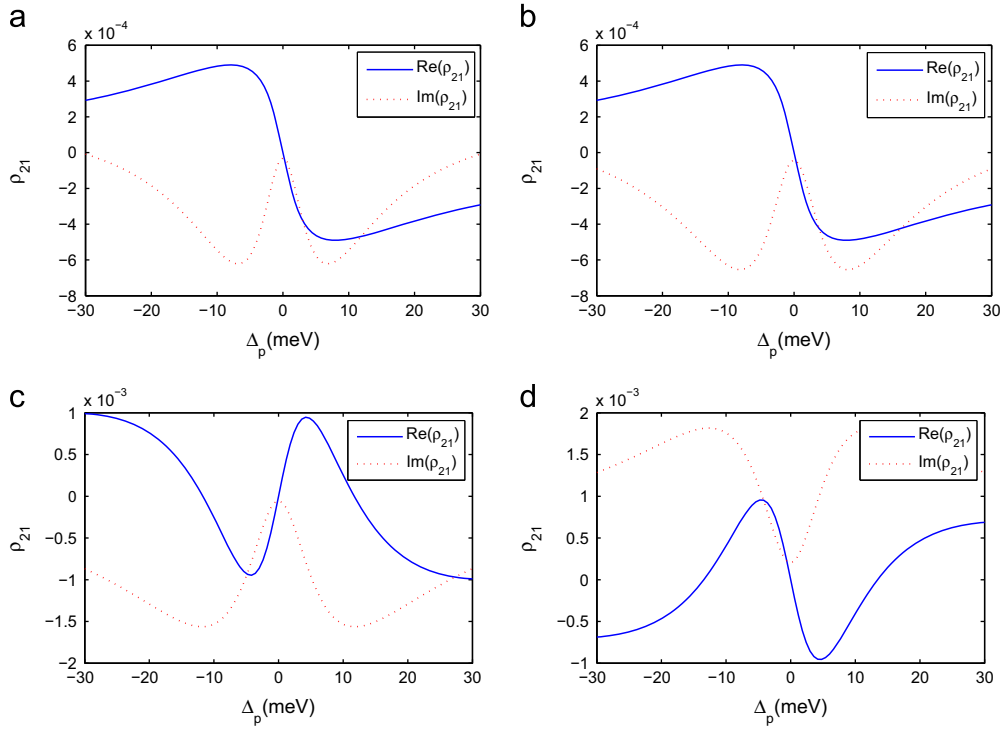

Fig. 4. The real (solid line) and imaginary (dotted line) parts of ρ_{21} as a function of the detuning of the probe field Δ_p with different cases: (a) $\phi=0$, $p=0$; (b)$\phi=\pi$, $p=0$; (c) $\phi=0$, $p=0.9$; (d) $\phi=\pi$, $p=0.9$. The other values of the parameters are chosen as $\Delta_L=\Delta_c=0$, $\gamma_2=1.32$ meV, $\gamma_3=1.72$ meV, $\gamma_4=2.24$ meV, $\gamma_{21}^{dph}=\gamma_{31}^{dph}=\gamma_{41}^{dph}=\gamma_{32}^{dph}=\gamma_{42}^{dph}=\gamma_{43}^{dph}=1.65$ meV, $\Omega_c=\Omega_L=\Omega=10$ meV, and $\Omega_p=0.1$ meV.

dispersion is accompanied with transparency at probing resonant position $\Delta_p = 0$ between two gain peaks, which presents the anomalous dispersion. This leads to the superluminal propagation of the probe field. When the relative phase ϕ is switched into π, one can find in Fig. 4(d) that the slope of dispersion becomes positive with transparency at probing resonant position $\Delta_p = 0$ between two absorption peaks, which presents the anomalous dispersion. That is, subluminal behavior occurs. In other words, due to the existence of the Fano interference, we can efficiently control the behavior of the dispersion and the group velocity of the weak probe field can be switched from superluminal to subluminal or vice versa by adjusting the relative phase ϕ between the two control fields.

For a better insight into the effects of the relative phase of the two control fields on the group velocity of the probe field, we now focus on the effects of the relative phase on the group index n_g. The present triple-coupled GaAs/AlGaAs SQW structure has been studied in several previous works [22,45,46]. The electron sheet density takes value $N = 10^{12}\ \mathrm{cm}^{-2}$. The value ensure that the system is initially in the lowest subband, so that the initial conditions can be satisfied in our numerical calculations (i.e., $\rho_{11}(0) = 1$, $\rho_{22,33,44}(0) = 0$). The dipole matrix element can be given as $\mu_{21} = e \times 3.4$ nm. Fig. 5 plots the curves of the group index n_g versus the relative phase ϕ under the condition of probing resonance, and it demonstrates that the group index has a strong dependence on the relative phase of the two control fields when $p \neq 0$. In the presence of the Fano-type interference, we can find from Fig. 5 that the curves of group index oscillate between positive values and negative values periodically as the relative phase changes, which implies that the group velocity of the weak probe field can be switched between subluminal and superluminal periodically. In addition, Fig. 5 clearly illustrates that oscillating amplitude of the phase-dependent group index is enhanced as Ω or p increases. In other words, low Rabi frequencies of the control fields and strength of the Fano interference induce less phase modulation of the group index, which can be well explained using the perturbation theory. Besides, we note that the period of phase dependence is approximately 2π.

4. The temporal and spatial dynamics of the probe pulse

Up to now, we have discussed how to control the group velocity of the probe field by adjusting some system parameters in the present SQW system. As illustrated in Figs. 2–5, the dispersion can be modulated from positive to negative values or vice versa by adjusting these parameters. At the same time, we can find that the absorption of the probe field can be negligible for a certain range of the probe detuning. Accordingly, the group velocity of the pulse propagating can be switched between subluminal and superluminal with transparency. In order to further study the pulse propagation in the present SQW system driven by the two coherent control fields, we now examine the propagating behavior of the probe pulse with a Gaussian-type envelope.

For a Gaussian pulse with pulse duration τ_p [11], the Maxwell wave equation under the slowly varying envelope approximation along the propagating direction z can be given as [38–40]

$$\frac{\partial \Omega_p(z,t)}{\partial z} + \frac{1}{c}\frac{\partial \Omega_p(z,t)}{\partial t} = i\kappa\rho_{21}(t), \tag{12}$$

where $\kappa_{21} = N\Omega_p|\mu_{12}|^2/(2\varepsilon_0\hbar c)$. For the convenience of analysis and numerical calculation, we take $\Omega_p(z,t) = \Omega_p g(z,t)$ with Ω_p the real constant describing the maximal value of Rabi frequency and $g(z,t)$ a dimensionless spatiotemporal pulse-shape function

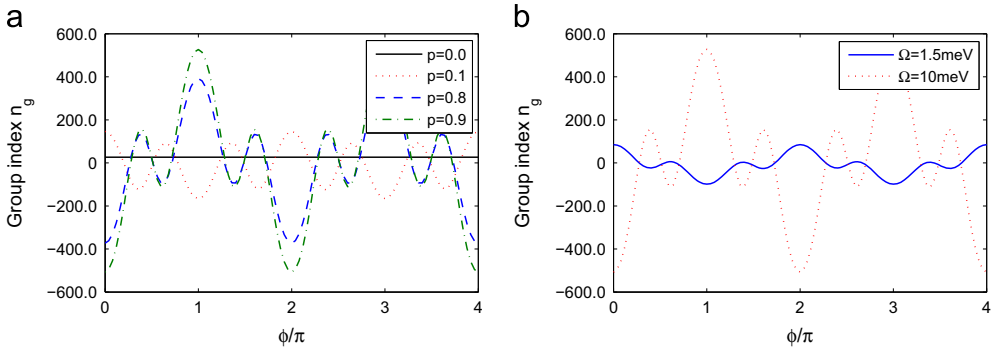

Fig. 5. The group index n_g as a function of the relative phase ϕ (a) with $\Omega_c = \Omega_L = \Omega = 10$ meV and different strengths of the Fano-type interference $p = 0$ (solid line), $p = 0.1$ (dotted line), $p = 0.8$ (dashed line), and $p = 0.9$ (dash-dotted line); (b) with $p = 0.9$ and different intensities of the two control fields $\Omega = 1.5$ meV (solid line) and $\Omega = 10$ meV (dotted line). The other values of the parameters are chosen as $\Delta_p = 0$, $\Delta_L = \Delta_c = 0$, $\gamma_2 = 1.32$ meV, $\gamma_3 = 1.72$ meV, $\gamma_4 = 2.24$ meV, $\gamma_{21}^{dph} = \gamma_{31}^{dph} = \gamma_{41}^{dph} = \gamma_{32}^{dph} = \gamma_{42}^{dph} = \gamma_{43}^{dph} = 1.65$ meV, and $\Omega_p = 0.1$ meV.

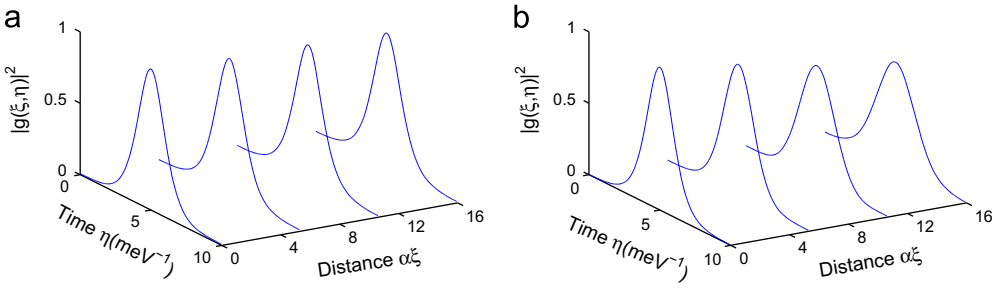

Fig. 6. The temporal and spatial evolution of the magnitude squared of the pulse envelopes with (a) $\phi = 0$ and (b) $\phi = \pi$. The other values of the parameters are chosen as $p = 0.9$, $\Delta_p = 0$, $\Delta_L = \Delta_c = 0$, $\gamma_2 = 1.32$ meV, $\gamma_3 = 1.72$ meV, $\gamma_4 = 2.24$ meV, $\gamma_{21}^{dph} = \gamma_{31}^{dph} = \gamma_{41}^{dph} = \gamma_{32}^{dph} = \gamma_{42}^{dph} = \gamma_{43}^{dph} = 1.65$ meV, and $\Omega_p = 0.1$ meV.

normalized by its peak value. By defining $\xi=z$ and $\eta=t-z/c$, Eq. (12) governing the pulsed probe field evolution can be written as

$$\frac{\partial g(\xi,\eta)}{\partial \alpha xi} = -i\frac{\gamma_{21}}{\Omega_p}\rho_{21}(\xi,\eta), \tag{13}$$

where the propagation constant on the left-hand side of the above equation is given by $\alpha=N\omega_p|\mu_{21}|^2/4\hbar\varepsilon_0 c\gamma_{21}$. In addition, the equations of motion for the density matrix elements $\rho_{ij}(\xi,\eta)$ can be rewritten according to Eqs. (1–9). Now we numerically solve Eqs. (13) and the density matrix equations with the same initial condition as in Fig. 4(c) and (d) and the boundary condition that the pulsed probe field is assumed as a Gaussian-type pulse at the beginning of the SQW system $\xi=0$. In Fig. 6, we show the result of numerical simulation on the Gaussian wave shape $|g(\xi,\eta)|^2$ with pulse duration $\tau_p=10$ meV$^{(-1)}$ versus the time η and distance $\alpha\xi$. It can be found from Fig. 6(a) that the SQW system is transparent to the resonant probe field which propagates over sufficiently long distances. The corresponding group velocity of the probe field can be calculated as $v_g=c/n_g=-5.7\times10^4$ m/s. When keeping all other parameters fixed but changing the relative phase ϕ from 0 to π, Fig. 6(b) illustrates that the absorption of the probe field increases slightly as the propagation distance increases. Accordingly, we obtain the group velocity of the probe field $v_g=c/n_g=5.4\times10^4$ m/s. Thus the pulsed probe field with Gaussian-type envelope can propagate through the present SQW system of length $16/\alpha$ with negligible distortion. Besides, the group velocity of the pulse propagation can be switched from superluminal to subluminal or vice versa via adjusting the relative phase between the two control fields. It is worth noting that the pulse distortion will appear as the propagation distance increases. However, the distortion-free propagation of the probe pulse can be also realized when the nonlinear effects of the system are included [38–40].

5. Conclusion

In conclusion, we have investigated the dispersion and the absorption of a weak probe pulse based on the ISBT in a triple semiconductor quantum well (SQW) structure driven coherently by two control laser fields. It is shown that the Fano-type interference and the Rabi frequencies of the control fields can modify the optical properties of the SQW structure. As a result, by properly tuning these parameters of the system, the group index of the probe pulse can be controlled efficiently and the group velocity of the light propagation can be switched between subluminal and superluminal. More interestingly, when the strong Fano-type interference is present, the dispersion and absorption properties become very sensitive to the relative phase of the two control fields. By adjusting this relative phase, the dispersion can be modified from positive to negative or vice versa, which leads to the propagation status of the pulse changing between subluminal and superluminal. Our calculations provide a guideline for optimizing and controlling the optical switching of the group velocity in the SQW solid-state system, which is much more practical than that in atomic system because of its flexible design and the controllable interference strength.

Acknowledgments

The research is supported in part by National Natural Science Foundation of China under Grant nos. 11374050 and 61372102, by Qing Lan project of Jiangsu, and by the Fundamental Research Funds for the Central Universities under Grant no. 2242012R30011.

References

[1] L.V. Hau, S.E. Harris, Z. Dutton, C.H. Behroozi, Nature 397 (1999) 594.
[2] M.O. Scully, Nature 426 (2003) 616.
[3] M.O. Scully, M.S. Zubairy, Science 301 (2003) 181.
[4] M.S. Bigelow, N.N. Lepeshkin, R.W. Boyd, Science 301 (2003) 200.
[5] M.S. Bigelow, N.N. Lepeshkin, R.W. Boyd, Phys. Rev. Lett. 90 (2003) 113903.
[6] Y. Wu, M.G. Payne, E.W. Hageley, L. Deng, Phys. Rev. A 69 (2004) 063803.
[7] Y. Wu, M.G. Payne, E.W. Hageley, L. Deng, Phys. Rev. A 70 (2004) 063812.
[8] D.F. Phillips, A. Fleischhauer, A. Mair, R.L. Walsworth, M.D. Lukin, Phys. Rev. Lett. 86 (2001) 783.
[9] M. Bajcsy, A.S. Zibrov, M.D. Lukin, Nature 426 (2003) 638.
[10] L.J. Wang, A. Kuzmich, A. Dogariu, Nature 406 (2000) 277.
[11] A. Dogariu, A. Kuzmich, L.J. Wang, Phys. Rev. A 63 (2001) 053806.
[12] D. Han, Y. Zeng, Y. Bai, H. Cao, W. Chen, C. Huang, H. Lu, Opt. Commun. 281 (2008) 4712.
[13] D. Han, Y. Zeng, Y. Bai, Opt. Commun. 284 (2011) 4541.
[14] G.S. Agarwal, W. Harshawardhan, Phys. Rev. Lett. 77 (1996) 1039.
[15] Y. Wu, M.G. Payne, E.W. Hagley, L. Deng, Opt. Lett. 29 (2004) 2294.
[16] Y. Wu, L. Deng, Opt. Lett. 29 (2004) 1144.
[17] S.E. Harris, Phys. Today 50 (1997) 36.
[18] H.C. Liu, F. Capasso, Intersubband Transitions in Quantum Wells: Physics and Device Applications, Academic, New York, 2000.
[19] Y. Wu, X. Yang, Appl. Phys. Lett. 91 (2007) 094104.
[20] A. Imamoglu, R.J. Ram, Opt. Lett. 19 (1994) 1744.
[21] J. Faist, F. Capasso, C. Sirtori, K. West, L.N. Pfeiffer, Nature 390 (1997) 589.
[22] C.R. Lee, Y.C. Li, F.K. Men, C.H. Pao, Y.C. Tsai, J.F. Wang, Appl. Phys. Lett. 86 (2005) 201112.
[23] M.D. Frogley, J.F. Dynes, M. Beck, J. Faist, C.C. Phillips, Nat. Mater. 5 (2006) 175.
[24] R. Atanasov, A. Hache, J.L.P. Hughes, H.M. van Driel, J.E. Sipe, Phys. Rev. Lett. 76 (1996) 1703.
[25] L. Silvestri, F. Bassani, G. Czajkowski, B. Davoudi, Eur. Phys. J. B 27 (2002) 89.
[26] P.C. Ku, F. Sedgwick, C.J. Chang-Hasnain, P. Palinginis, T. Li, H. Wang, S.W. Chang, S.L. Chuang, Opt. Lett. 29 (2004) 2291.
[27] J. Faist, C. Sirtori, F. Capasso, S.N.G. Chu, L.N. Pfeiffer, K.W. West, Opt. Lett. 21 (1996) 985.
[28] G.B. Serapiglia, E. Paspalakis, C. Sirtori, K.L. Vodopyanov, C.C. Phillips, Phys. Rev. Lett. 84 (2000) 1019.
[29] E. Paspalakis, M. Tsaousidou, A.F. Terzis, Phys. Rev. B 73 (2006) 125344.
[30] P.I. Tamborenea, H. Metiu, Phys. Lett. A 240 (1998) 265.
[31] H. Sun, S. Fan, H. Zhang, S. Gong, Phys. Rev. B 87 (2013) 235310.
[32] J.H. Li, Phys. Rev. B 75 (2007) 155329.
[33] Z. Wang, S. Zheng, X. Wu, J. Zhu, Z. Cao, B. Yu, Opt. Commun. 304 (2013) 7.
[34] A. Joshi, M. Xiao, Appl. Phys. B 79 (2004) 65.
[35] Y. Xue, X.M. Su, G. Wang, Y. Chen, J.Y. Gao, Opt. Commun. 249 (2005) 231.
[36] J.H. Wu, J.Y. Gao, J.H. Xu, L. Silvestri, M. Artoni, G.C. La Rocca, F. Bassani, Phys. Rev. Lett. 95 (2005) 057401.
[37] J.H. Wu, J.Y. Gao, J.H. Xu, L. Silvestri, M. Artoni, G.C. La Rocca, F. Bassani, Phys. Rev. A 73 (2006) 053818.
[38] W.X. Yang, J.M. Hou, R.K. Lee, Phys. Rev. A 77 (2008) 033838.
[39] W.X. Yang, J.M. Hou, Y.Y. Lin, R.K. Lee, Phys. Rev. A 79 (2009) 033825.
[40] W.X. Yang, R.K. Lee, EuroPhys. Lett. 83 (2008) 14002.
[41] M. Shapiro, P. Brumer, Rep. Prog. Phys. 66 (2003) 859.
[42] J.F. Dynes, E. Paspalakis, Phys. Rev. B 73 (2006) 233305.
[43] S.M. Goodnick, P. Lugli, in: J. Shah (Ed.), Hot Carriers in Semiconductor Nanostructures, Academic, San Diego, 1992, p. 219 (Chapter 3).
[44] W. Potz, Phys. Rev. B 71 (2005) 125331.
[45] E. Voutsinas, A. Fountoulakis, A.F. Terzis, J. Boviatsis, S. Baskoutas, E. Paspalakis, Proc. SPIE 6321 (2006) 63210P.
[46] J. Li, X. Hao, J. Liu, X. Yang, Phys. Lett. A 372 (2008) 716.
[47] F. Biancalana, S.B. Healy, R. Fehse, E.P. OReilly, Phys. Rev. A 73 (2006) 063826.
[48] I. Waldmüller, J. Forstner, S.-C. Lee, A. Knorr, M. Woerner, K. Reimann, R.A. Kaindl, T. Elsaesser, R. Hey, K.H. Ploog, Phys. Rev. B 69 (2004) 205307.